The Implementation of a Dual Wound Machine Using a Fractional Slot Winding

C G Hodge OBE MSc CEng CMarEng HonFIMarEST FREng*!
B Yin BEng#
X Pei PhD MSc BEng CEng#
J F Eastham Dr. h.c. DSc FIET FRSE FREng#
X Zeng PhD MSc BEng#
O J Simmonds MEng MSc CEng CMarEng MIMechE MIMarEST*

* BMT, UK
# University of Bath, UK
! Corresponding Author - Email: c.hodge@imarest.org. [1]

Synopsis

The benefits to be gained from high and directed energy weapons make them attractive, however they will require further electrification of warships. An important design requirement for the resultant total power system will be to achieve close integration between the weapons' and ship's power system segments, accounting for their differing time constants and establishing high levels of segregation and decoupling to minimise disturbances moving between the two segments. Above all the need to minimise cost and weight will dominate the design and its acceptability. A dual wound machine with two windings contained in the same stator slots, but nevertheless electrically isolated and magnetically decoupled from each other, will solve much of the system design challenge. The machine, employed as an alternator, with two independent outputs, one for each use, and yet driven by a single prime mover, and with little impact on overall length, will be highly attractive and may simplify the retrofit of high and directed energy weapons in mechanically propelled warships.

This paper describes the general background to a dual wound machine winding design including the calculation of its magnetic space harmonics, the requirements necessary to achieve magnetic decoupling between the two windings, and those to avoid unbalanced magnetic pull. These considerations lead to a dual winding of four and eight poles being the lowest pole numbers that give a practicable winding.

The paper then continues to describe a specific four and eight pole dual winding design aimed at installation on an existing laboratory machine at the University of Bath. Once rewound it is intended that the machine will serve as a small-scale demonstrator. The machine has 36 slots and while the four-pole winding can be achieved as an integral slot winding the eight-pole winding is by necessity fractional.

The resulting dual winding space harmonics are calculated by algebra and by a powerful computer method and these are used to demonstrate that the main pole face fluxes of the two windings do not couple magnetically. The winding is also analysed by two-dimensional flux modelling which confirms the main pole flux isolation and demonstrates that the tooth leakage flux does not lead to any loss of magnetic decoupling.

The demonstration that the end turn leakage flux does not lead to magnetic coupling between the two windings is left as one of the key design aspects to be demonstrated by the small-scale demonstrator.

Keywords: Electric Propulsion, Generators, Space Harmonics, Magnetic Coupling

1. Introduction

High and directed energy weapon systems such as lasers, along with aircraft and drone electromagnetic launch are now in service and further developments are proceeding to increase the laser power and therefore its effectiveness. The resulting increase in electrical power demand will exacerbate the difficulty of the design of the power system and challenge the limits on volume and weight arising from the ship's naval architecture. Previous papers by two of the authors, (Eastham & Hodge, 2015; Hodge & Eastham, 2015, 2015 & 2016) , have described a novel stator design with two independent windings, wound in the same stator slots, yet electrically isolated and

[1]

Christopher Hodge is the Chief Electrical Engineer at BMT Defence & Security (UK) Ltd
Boyuan Yin is a Research Student in the Department of Electrical Engineering at the University of Bath
Xiaoze Pei is an Assistant Professor in the Department of Electrical Engineering at the University of Bath
Fred Eastham is an Emeritus Professor of Electrical Engineering at the University of Bath
Xianwu Zeng is an Assistant Professor in the Department of Mechanical Engineering at the University of Bath
Oliver Simmonds is a Principal Electrical Engineer at BMT Defence & Security (UK) Ltd

 https://doi.org/10.24868/issn.2515-818X.2020.045

magnetically decoupled. Such a machine, termed a Dual Wound Machine, will provide complete isolation between the weapons and ships services segments of the power system making the overall system very much easier to design. The resulting system would be more robust but would still retain the benefits of integrated power systems and will allow the adoption of the electric war ship concept in smaller ships than have so far been considered.

This paper first describes the machine held at the at the University of Bath which is intended to serve as a scaled dual wound machine demonstrator. The analysis of the spatial MMF harmonics and the determination of the requirements to avoid unbalanced magnetic pull in the dual wound machine presence are then described and the resulting practical winding configuration defined and its MMF profiles illustrated. The paper then summarises the two-dimensional flux modelling that was conducted by the University of Bath which confirmed the initial analysis of magnetic decoupling between the two windings. After which the paper finishes by considering the remaining testing programme that will be necessary to fully validate the concept of a dual wound machine.

2. The University of Bath Demonstration Machine

A laboratory machine, as detailed at Table 1, at the University of Bath is to be used as a small scale dual wound machine demonstrator. It currently has universal windings on the stator and rotor with all coil connections, both rotor and stator, externally accessible and straightforwardly reconfigurable. Nevertheless, in order to achieve a practicable dual winding (see later), and to reduce the presence of unwanted excitation space harmonics, both the stator and rotor will need rewinding. The machine is mounted on a dedicated bedplate and is directly coupled to a DC machine fed from a VARIAC and rectifier, which will drive the demonstration machine, once it is rewound, as an alternator. The stator and the rotor of the donor machine are shown at Figure 1.

Table 1: Details of Existing Donor AC Machine

Speed	3000 RPM
Line Voltage	200 V
Line Current	14.5 A
Power	5 kVA
Frequency	50 Hz
Phase	3
Power factor	0.8
Excitation Voltage	25 V
Excitation Current	11.4 A
Stator Slots	36
Rotor Slots	24

After the rewind both windings will be star connected and produce 202 V phase voltage, 350 V line voltage. The four-pole winding will be rated at 6.45 A and 3.91 kVA and the eight-pole winding will be rated at 2.9 A and 1.76 kVA.

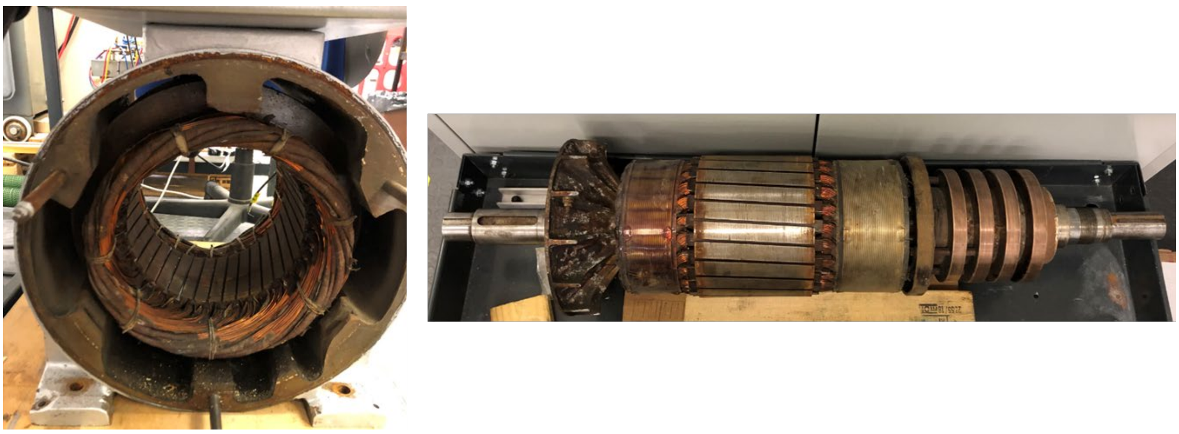

Figure 1: University of Bath Donor Machine Stator and Rotor

The winding patterns to be used will be described but first the method of achieving no magnetic coupling and no overall unbalanced magnetic pull when the two stator windings are energised will be explained.

 https://doi.org/10.24868/issn.2515-818X.2020.045

4. Magnetic Decoupling

As is explained in the earlier papers by two of the authors, (Eastham & Hodge, 2015; Hodge & Eastham, 2015, 2015 & 2016), to identify whether any coupling between the two windings exists it is necessary to consider the spatial distribution of the flux density around the air gap and the space harmonics that it contains. Because the relative permeability of iron, below saturation, is approximately 200,000, the Magnetomotive Force (MMF) dropped in the iron can be ignored compared to that dropped across the air gap. With this simplification half the total MMF is dropped on each of the two occasions that the flux passes across the air gap. If saturation is ignored the result is that the air-gap flux density will be proportional to the MMF dropped across the air gap and therefore the airgap flux density and the MMF will have the same shape and contain the same harmonics and in the same proportions. This considerably simplifies the derivation and analysis of a winding's MMF space harmonics if content and relative magnitude are all that is needed. This is the case in this present consideration and therefore a sufficient knowledge of the air gap MMF can be developed from a simple knowledge of the spatial distribution of the conductors. For example, Figure 2 shows the cross section through a rotor and a stator with one coil and the MMF profile that it develops.

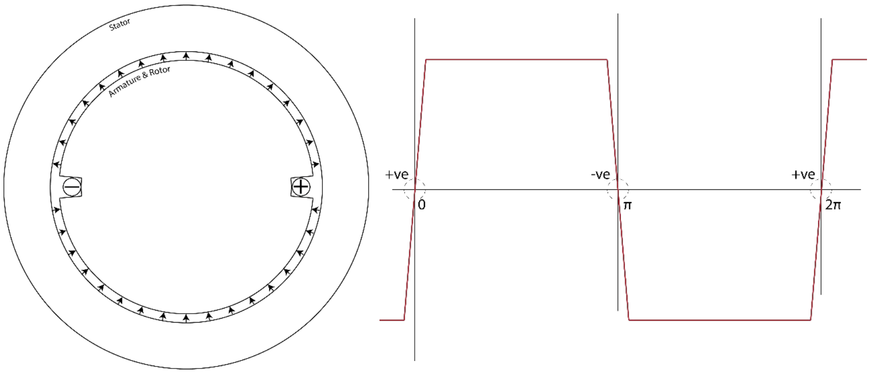

Figure 2: A Single Coil and its Spatial; MMF Distribution

Figure 3 shows the coil's space harmonics (plotted spatially as sinusoids) and the reconstruction from those harmonics of the coil's spatial distribution. In other words the spatial distribution of the coil shown on the left hand side of Figure 2 has been represented as a series of space harmonics, each being a simple sinusoid containing magnitude and phase information. The step from the space harmonics of the coil to the space harmonics of the MMF is achieved by an application of Ampere's rule and simply requires spatial integration (integration with respect to angle) of the coil harmonics which, being themselves simple sinusoids, is straightforward.

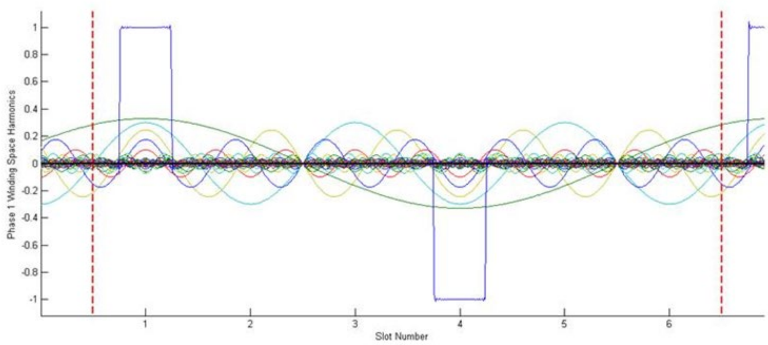

Figure 3: Space Harmonics of a Single Coil and its Reconstruction

 https://doi.org/10.24868/issn.2515-818X.2020.045

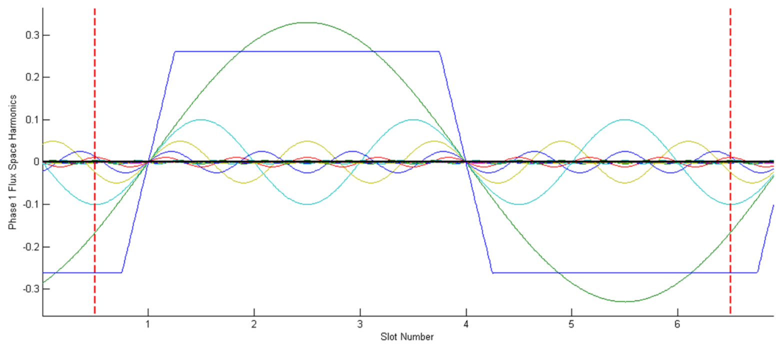

Figure 4: MMF Space Harmonics of a Single Coil and its Reconstruction

Figure 4 shows the MMF profile for the single coil reconstructed from its space harmonics gained by spatial integration of the coil space harmonics shown in Figure 3.

The spatial harmonic content for any winding distribution is simply extracted by using whatever form of the Fourier series is convenient and taking account of all the conductors in a phase. This then leads directly to the spatial harmonics of the phase MMF just as has been described.

Once the MMF arising from each phase is known the total MMF can be determined by combining each phase's harmonics together once they have been scaled to take account of the electrical supply angle and the resulting relative loading of each phase. Individual harmonics can be thought of as phasors and those of the same order are combined in the usual fashion, either using complex notation to hold the phase information, or by standard trigonometry.

Once the unified single air gap MMF (and magnetic flux density) harmonics are obtained for each of the windings in the dual wound machine then the test for magnetic decoupling is straight forward: it arises when the two windings have no space harmonics in common.

5. Unbalanced Magnetic Pull

Having no unbalanced magnetic pull (UMP) is the second key design criteria that the authors have sought to fulfil along with no magnetic coupling between the windings. It is possible that some UMP could be accommodated with specially rated bearings but in the context of the anticipated use in a warship, high reliability and low noise and vibration are sensible aspirations which will be supported by avoiding UMP. The analysis for UMP proceeded in two ways. First the UMP of the proposed dual wound machine was calculated from the total air gap MMF profile by a Matlab programme. Second a general algebraic approach was applied but confined to a flux produced by the combination of the fundamental MMF profiles for the two windings. This simplification made the algebra, and its various integrations and trigonometric manipulations, tractable.

In each method the UMP force density (force per Amp per unit circumferential length) was taken as being proportional to the square of the flux density passing through the air gap, and the force was taken as being directed radially inwards. This was, in essence, the force on the stator, it could of course quite equally have been calculated with the force being directed radially outwards to give the force on the rotor. (Newton's third law.)

The first method used Matlab to calculate the overall UMP by multiplying the force density by the angular step used in the derivation of the MMF profile, resolving it into vertical and horizontal components and summing these around the full circumference.

The second method, using fundamental MMF distributions only, performed the same process, but through algebra, with the final summation achieved by integration.

Both methods gave the same result; to avoid UMP the pole numbers in the two windings must differ by more than one pole-pair (two poles). So, for example, 2 and 3 pole-pairs (4 and 6 poles) would have UMP whereas 2 and 4 pole-pairs (4 and 8 poles) would not.

 https://doi.org/10.24868/issn.2515-818X.2020.045

7. The Demonstrator Machine Windings

7.1. Stator Windings

The stator of the demonstrator machine has thirty-six slots, which is insufficient to merge the two windings circumferentially in two layers. Adopting a four-layer winding (radial merging) will allow each winding to use the full 36 slots in two layers but even then, high pole numbers will be difficult to wind in only 36 slots. In addition, the pole-pair numbers in the two windings must differ by at least two and not share any space harmonics. The possibilities are assessed in Table 2.

Table 2: Assessment of Possible Winding Pole Numbers

Pole-Pairs		Slots per Pole per Phase		Comment
Winding 1	Winding 2	Winding 1	Winding 2	
1	2	6	3	UMP present.
1	3	6	2	No UMP, no space harmonics in common
1	4	6	1.5	Space Harmonics in common.
2	3	3	2	UMP present, space harmonics in common.
2	4	3	1.5	No UMP, no space harmonics in common.

The choice was therefore between a 1/3 and a 2/4 pole-pair winding. Both these windings have acceptably low pole-numbers, no UMP and no space harmonics in common. Both the resulting dual windings are capable of being implemented in 36 slots although the four pole-pair winding suffers slightly from necessarily being a fractional slot winding. Despite this, the 2/4 pole-pair winding was chosen as it simplifies the end winding geometry in the restricted space available in the demonstration machine. Fractional slots windings and their space harmonics were considered by two of the authors in an earlier paper (Eastham & Hodge, 2015) and this confirms that the four pole-pair winding will serve well in the demonstration machine. The full winding patterns for the two pole-pair and four pole-pair windings, each in two layers and 36 slots are shown at Figure 5.

Four Pole-Pair	Layer 4	R	R	b	Y	Y	r	B	B	y	R	R	b	Y	Y	r	B	B	y
	Layer 3	b	b	Y	r	r	B	y	y	R	b	b	Y	r	r	B	y	y	R
Two Pole-Pair	Layer 2	R	R	R	b	b	b	Y	Y	Y	r	r	r	B	B	B	y	y	y
	Layer 1	b	b	b	Y	Y	Y	r	r	r	B	B	B	y	y	y	R	R	R
Slot Number		1	2	3	4	5	6	7	8	9	10	11	12	13	14	15	16	17	18

Four Pole-Pair	Layer 4	R	R	b	Y	Y	r	B	B	y	R	R	b	Y	Y	r	B	B	y
	Layer 3	b	b	Y	r	r	B	y	y	R	b	b	Y	r	r	B	y	y	R
Two Pole-Pair	Layer 2	R	R	R	b	b	b	Y	Y	Y	r	r	r	B	B	B	y	y	y
	Layer 1	b	b	b	Y	Y	Y	r	r	r	B	B	B	y	y	y	R	R	R
Slot Number		19	20	21	22	23	24	25	26	27	28	29	30	31	32	33	34	35	36

Figure 5: 2/4 Pole-Pair Dual Winding in Four Layers and Thirty-Six Slots

In Figure 5 the letters (and colours) indicate the three phases, upper case letters denote positively directed current and lower case letters denote negatively directed current. The two pole-pair winding has three slots per pole per phase and the four pole-pair winding has 1.5 slots per pole per phase. Importantly the three phases in each pair of layers are electrically isolated and operate at different frequencies. The MMF distributions arising from the two separate windings and the overall dual winding are shown in Figure 6.

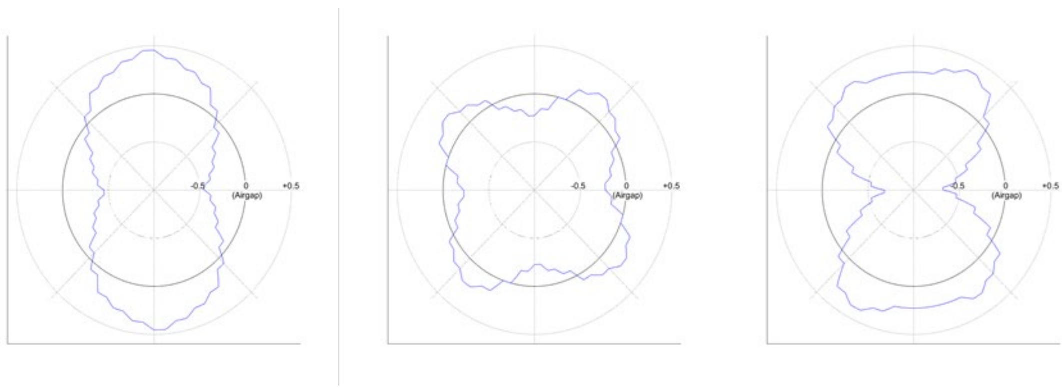

Figure 6: Air Gap MMF Plots for the Two and Four Pole-Pair Windings and for the Dual Winding Stator

https://doi.org/10.24868/issn.2515-818X.2020.045

The plots in Figure 6 are not polar plots; the origin is not the centre of the plot. Zero MMF lies on the black circle, MMF beneath that is “negative” and MMF above “positive”. If a true polar plot were used much of the visible plot would overlap with its opposite sign MMF (+1 at 30º and -1 at 210º is the same point on a polar plot). The air gap plot gives a good visual representation of the MMF around the air gap and the flux density that it produces. The heights of the MMF curve indicate the flux density at the air gap, and therefore inevitably some distortion results because the absolute size of an arc varies with radius and this leads to the total negative flux appearing to be smaller than the total positive flux (these total fluxes are the areas beneath and above the zero MMF circle respectively). The MMF plots in Figure 6 have been drawn for a zero electrical supply angle.

7.2. Stator Winding MMF Space Harmonics

The stator winding MMF space harmonics for its two and four pole-pair windings are listed in Table 3.

Table 3: Stator Windings MMF Space Harmonics

Harmonic	2 Pole-Pair	4 Pole-Pair
2	1.0000	
4		0.4981
8		0.0453
10	0.0440	
14	0.0248	
16		0.0261
20		0.0199
22	0.0144	
26	0.0139	
28		0.0102
32		0.0441
34	0.0396	
38	0.0317	
40		0.0282
44		0.0041
46	0.0045	
50	0.0028	0.0000

Harmonic	2 Pole-Pair	4 Pole-Pair
52		0.0029
56		0.0021
58	0.0014	
62	0.0011	
64		0.0007
68		0.0017
70	0.0008	
74	0.0007	
76		0.0014
80		0.0005
82	0.0007	
86	0.0007	
88		0.0009
92		0.0009
94	0.0008	
98	0.0010	
100		0.0007

In Table 3 the amplitude of the harmonics have been referenced to the amplitude of the fundamental of the two pole-pair winding and, to save space, phase information has not been included because the main purpose is to determine whether the two windings have any space harmonics in common.

7.3. The Rotor Windings

The rotor has 24 slots. It needs to have two DC field systems, one four-pole and one eight-pole, both can be wound concentrically. Again the windings will be wound on top of each other, each using all the 24 slots. In order to produce as close to a sinusoidal spatial distribution of flux the numbers of conductors in each slot have been varied sinusoidally. The pattern of conductors in the coils in each rotor winding are now described:

7.3.1. Four Pole:

The pattern for the four-pole DC rotor winding for each coil side is $[450\ 329\ 121]^{+ve}$ and $[121\ 329\ 450]^{-ve}$. This covers six slots and is repeated three further times, with the polarity alternating to produce four poles in 24 slots. This is illustrated in Figure 7.

 https://doi.org/10.24868/issn.2515-818X.2020.045

			P1						P2						P3						P4			
			↑						↓						↑						↓			
Conductor Numbers	450	329	121	121	329	450	450	329	121	121	329	450	450	329	121	121	329	450	450	329	121	121	329	450
Four Pole																								
Slot Number	1	2	3	4	5	6	7	8	9	10	11	12	13	14	15	16	17	18	19	20	21	22	23	24

Figure 7: Four Pole DC Winding in 24 Slots with Sinusoidally Distributed Conductors

7.3.2. Eight-Pole

The pattern used for the eight-pole winding is similar, again the conductors are sinusoidally distributed, and the pattern is [230 190]$^{+ve}$ and [190 230]$^{-ve}$. This covers four slots and is repeated a further seven times to produce eight poles but nominally in 32 slots. The winding is reduced to 24 slots by combining the sixteen slots with 230 conductors into eight slots with 460 conductors. This is illustrated in Figure 8 but note that Slot 1 appears twice with half its conductors in each instance, shown as 460/2.

		P1			P2			P3			P4			P5			P6			P7			P8		
		↑			↓			↑			↓			↑			↓			↑			↓		
Conductor Numbers	460/2	190	190	460	190	190	460	190	190	460	190	190	460	190	190	460	190	190	460	190	190	460	190	190	460/2
Eight Pole																									
Slot Number	1	2	3	4	5	6	7	8	9	10	11	12	13	14	15	16	17	18	19	20	21	22	23	24	1

Figure 8: Eight Pole DC Winding in 24 Slots with Sinusoidally Distributed Conductors

The rotor winding distributions can be analysed in the same way as the stator windings

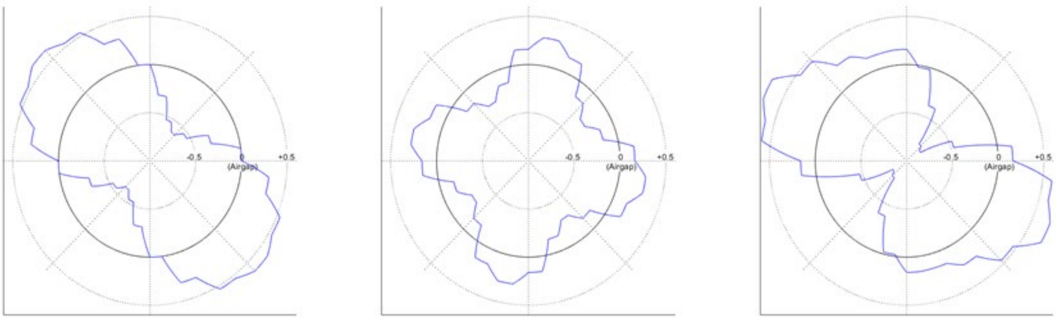

Figure 9: Air Gap MMF Plots for the Two and Four Pole-Pair Windings and for the Dual Winding Rotor

7.4. Rotor Winding MMF Space Harmonics

The rotor winding MMF space harmonics for its two and four pole-pair windings are listed in Table 4.

https://doi.org/10.24868/issn.2515-818X.2020.045

Table 4: Rotor Windings MMF Space Harmonics

Harmonic	2 Pole-Pair	4 Pole-Pair
2	1.000000	
4		0.461222
8		0.000162
10	0.000189	
12		0.017232
14	0.000126	
20		0.068852
22	0.062775	
26	0.044945	
28		0.035129
34	0.000021	
36		0.001915
38	0.000013	
44		0.003812
46	0.001890	
50	0.001600	

Harmonic	2 Pole-Pair	4 Pole-Pair
52		0.002729
56		0.000008
58	0.000006	
60		0.000689
62	0.000006	
68		0.005956
70	0.006201	
74	0.005548	
76		0.004768
82	0.000004	
84		0.000352
86	0.000003	
92		0.000872
94	0.000453	
98	0.000416	
100		0.000738

These harmonics are again rationalised to the magnitude of the fundamental of the four-pole winding. The harmonics are written to six decimal places because the higher harmonics are much smaller than the equivalent harmonics for the stator MMF distribution which were written to four decimal places. Even so some rotor MMF space harmonics which do exist do not appear when written to six decimal places and have been excluded. Since they are around a millionth of the amplitude of the fundamental, they do not contribute much and their exclusion allows higher order harmonics with an amplitude visible in the sixth decimal place to be listed without taking up more space.

7.5. Stator and Rotor Dual Winding Coupling

From Table 3 it is immediately apparent that the two stator windings have no space harmonics in common and they will therefore not couple magnetically. Similarly, Table 4 shows that the two rotor windings will not couple magnetically. Transient load disturbances will not be passed between the two supplies.

7.6. Rotor Stator Cross Coupling

Importantly, taken together, Table 3 and Table 4 show that the two pole-pair rotor winding has no harmonics in common with the four pole-pair stator winding illustrating that for both transient and steady state variation in the two pole-pair excitation current there will be no induced EMF changes in the four pole-pair stator winding. The same holds for the four pole-pair rotor excitation current and the two pole-pair stator winding. There is therefore no control cross-coupling between the two supplies.

8. Finite Element Flux Modelling

The preceding analysis provides confidence that the two windings will be decoupled. However, the analysis takes no account of slot leakage or end-turn leakage (pole face leakage cannot affect harmonic coupling). A two-dimensional finite element flux plot of the dual wound machine was undertaken, using COMSOL, to take account of slot leakage and to validate the preceding harmonic analysis leakage. The two-dimensional analysis cannot take account of end turn leakage which will require three-dimensional flux modelling which is not currently available to the authors. However, the demonstrator will establish the impact of any end turn affects as well as provide assurance for the two-dimensional finite element analysis. As an example of the FE model's output is at Figure 10.

 https://doi.org/10.24868/issn.2515-818X.2020.045

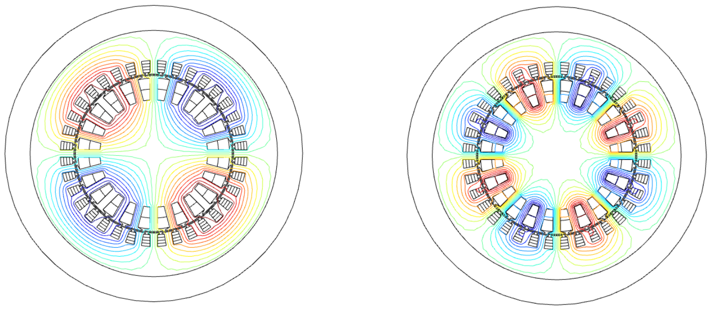

Figure 10: Magnetic Vector Potential Plot, Four Pole and Eight Pole Rotor Excitation

The Finite Element Analysis provided a wide range of information including voltage profiles and selection of the optimum displacement between the four and eight pole windings, however the key aspect of this paper is the presence or otherwise of any magnetic coupling between the two windings. The first test to see if any coupling existed was to excite the four pole and eight pole rotor windings, in turn, through the FE model and to determine whether any voltage appeared on the opposite stator winding.

The effect of rotor four-pole winding excitation on the stator voltages is shown in Figure 11.

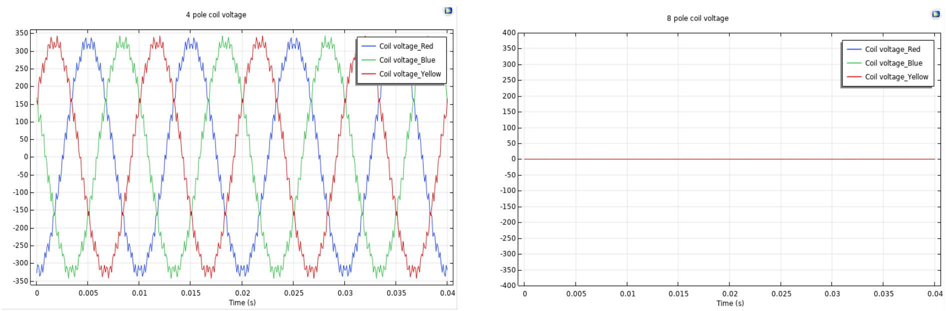

Figure 11: Stator Winding Voltages due to Four Pole Rotor Excitation

The effect of eight-pole rotor winding excitation on the stator voltages is shown in Figure 12.

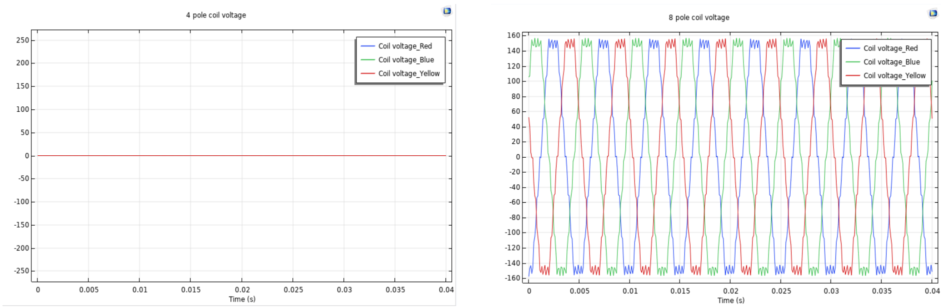

Figure 12: Stator Winding Voltages due to Eight Pole Rotor Excitation

These clearly demonstrated the lack of magnetic coupling between the four and eight pole fields. Finally, with respect to magnetic decoupling, the FE model was exercised further to investigate whether any transient caused by load changes reflected across the winding sets. The limitations of COMSOL required the FE to be conducted under steady state conditions so three situations were simulated, all with both the 4 pole and 8 pole rotor windings energized:

Test 1

- 4 pole stator winding feeding 34 Ω resistive load.
- 8 pole stator winding open circuit.

Test 2

- 4 pole stator winding open circuit.
- 8 pole stator winding feeding 13 Ω resistive load.

 https://doi.org/10.24868/issn.2515-818X.2020.045

Test 3

- 4 pole stator winding with 34 Ω resistive load.
- 8 pole stator winding with 13 Ω resistive load.

The voltage and current waveforms developed in the third test were identical with those developed in the earlier tests when the opposite winding was unloaded for which the voltage variations are shown at Figure 11 for the four-pole voltage and Figure 12 for the eight-pole voltage. This confirmed the earlier demonstration of the absence of magnetic coupling between the four and pole windings.

9. Further Testing

The initial algebraic and computer analyses produced no coupling due to the main air-gap flux, however it did not take account of either slot leakage flux or end turn leakage flux. The two-dimensional FE analysis provided confidence that the tooth leakage flux would not lead to any magnetic coupling but still did not take account of the end turn leakage. The decision to use the existing laboratory machine as a small scale demonstrator was, at least in part, made in order to determine whether end turn leakage affected the overall magnetic isolation of the two windings.

The testing programme is now being developed and it will include the usual phases:

- Construction and build integrity verification.
- Electrical connections verification.
- Initial test machine rotation at increasing speeds up to the design speed and over-speed.
- Excitation of the stator windings, separately and together.
- Steady state progressive loading of the stator windings, separately and together

The crux of the testing will then follow as both windings are excited, load changes imposed, and a search conducted for evidence of any coupling between the two stator windings or any changes in the current of a first excitation winding producing emf in the second stator winding.

10. Conclusion

The advantages to be gained from using a dual wound generator to provide weapon and ship service power have been stated and the design process that has been undertaken to identify a suitable dual winding combination has been described. Although the final implementation of the proposed dual wound machine demonstrator has yet to be completed, and its testing undertaken, nothing that has so far been conducted in any of the analyses, algebraic, computer based and finite element, has shown anything other than that the machine will work well in providing two independent supplies with complete electrical and magnetic isolation.

The authors remain confident that a dual wound alternator is a practical and a practicable proposition.

References

Eastham JF, Hodge CG, “Fractional-Slot Windings and their Space Harmonics”, Proceedings of the Engine as a Weapon Symposium, Bath, UK, June 23 – 24 2015.

Hodge CG, Eastham JF, “Dual Wound Machines for Electric Ship Power Systems”, Proceedings of the Electric Ship Technologies Symposium, Alexandria VA|, USA, June 22 – 24 2015.

Hodge CG, Eastham JF, “Machine Spatial Air Gap Flux Density Analysis”, Proceedings of the World Maritime Technology Conference, Providence RI, USA, November 3 – 7 2015.

Hodge CG, Eastham JF, “The Cancellation of Dual Winding Harmonic Coupling by Winding Design”, Proceedings of the International Naval Engineering Conference, Bristol, UK, April 26 – 28 2016.

 https://doi.org/10.24868/issn.2515-818X.2020.045